



Design and tolerances of the cold bore / beam screen with shielding

C. Garion
CERN/TE/VSC



with contribution of R. Fernandez Gomez, H. Kos, M. Morrone, H. Rambeau, A. Vidal

Outline

- Functional requirements
- HL-LHC beam screen concept
 - Design criteria
 - Boundary conditions
 - Material properties
- Thermal mechanical study
 - Mechanical design
 - Model
 - Q2-Q3, D1, Q1 designs
 - Heat transfer
 - Thermal analysis of the thermal links
 - Mechanical consideration for the thermal links
 - Supporting system
- Nominal dimensions and tolerances
 - Components
 - Assembly
- Prototyping
- Summary

Functional requirements

Conceptual specification: EDMS 1361079.

“This component ensure the vacuum performance together with shielding the cold mass from physics debris and screening the cold bore cryogenic system from beam induced heating.

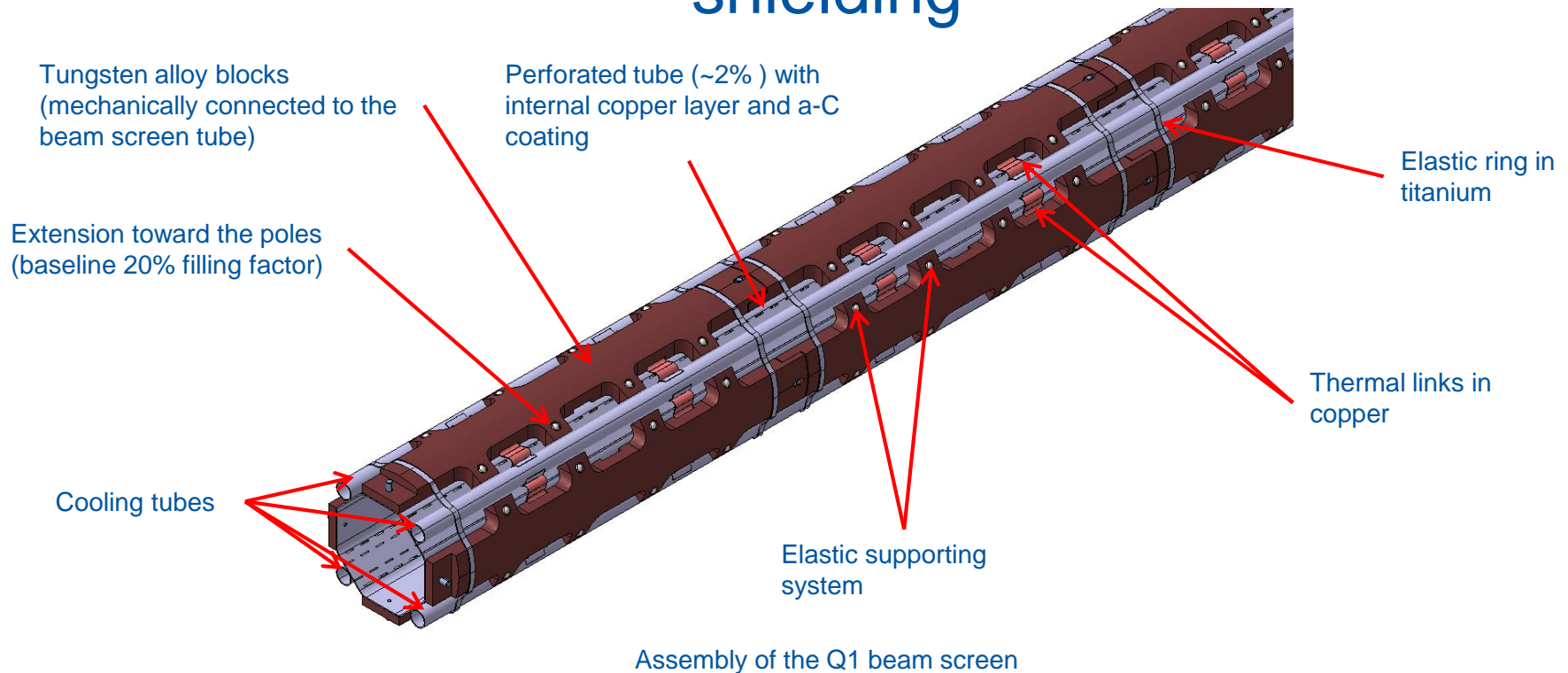
*The shielded beam screen has to withstand the Lorentz forces induced by eddy currents during a quench. **50 cycles at high field.** (13th HL-LHC TC)*

*The temperature of the shielded beam screen must be actively controlled in a given temperature range: **40-60 K.** (Temperature window to be confirmed)*

The system must be compatible with impedance performances.

The system must be compatible with the machine aperture.”

Concept of the HL-LHC beam screen with shielding



1. Tungsten block mechanically connected to the beam screen

➤ Positioning pins

- Pins are positioned and welded to the beam screen
- Inermet blocks are positioned thanks to the pins
 - Dedicated slots are used on one side to allow the differential thermal contraction
 - An overlap is used to reduce the number of pins

➤ Blocks are maintained in position with elastic rings

2. Copper based strips for the heat transfer to the cooling tubes

Mechanical design criteria and boundary conditions

The cold bore shall fulfil several requirements:

- Mechanical stability under external pressure
- Elastic behaviour: equivalent stress lower than the yield strength
- Limited deformation to avoid interference with the magnet coils

The beam screen integrity shall be ensured during a magnet quench:

- Elastic behaviour of the beam screen wall
- Limited plastic strain of the copper layer
- Limited stress at the interface between the copper layer and the beam screen wall

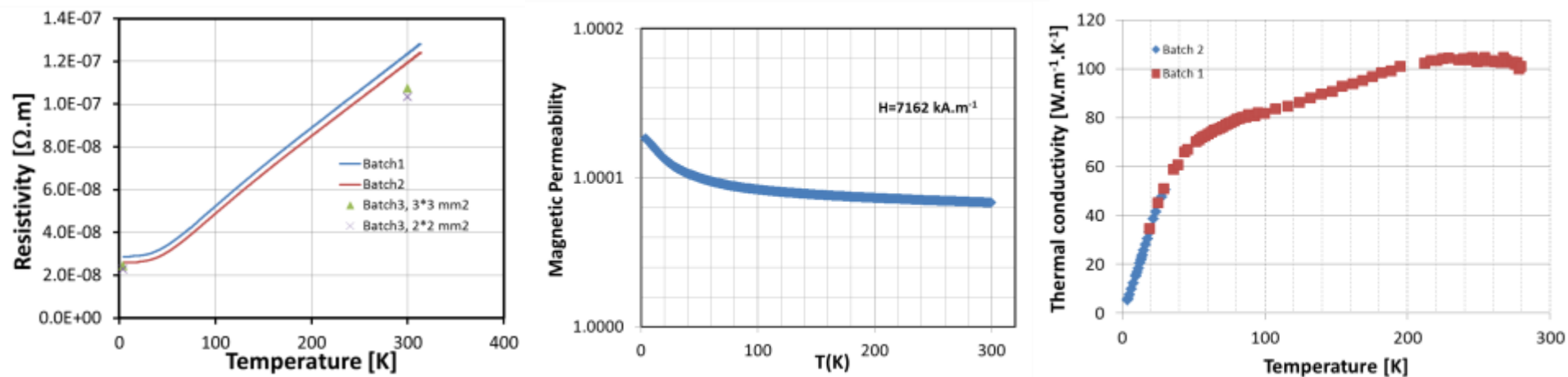
The boundary conditions for the design are:

- Nominal magnetic field and gradient: 5.6 T (D1), 140 T.m⁻¹ (Q1-Q3)
- Coil inner diameter: ~150 mm (more details in slide 24)
- Design pressure for the cold bore: 20 bars ext.
- Shielding thickness of 16 mm for the Q1, 6 mm for the other magnets
- Heat load: 20 W.m⁻¹ (beam screen)
- Temperatures:
 - Beam screen: 40-60 K
 - Cold bore: 1.9 K

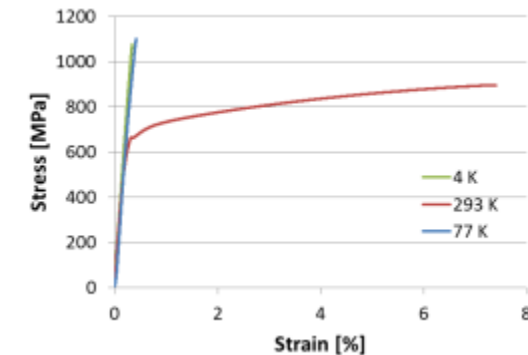
Material properties

Inermet® 180

Some physical properties have been measured.



Mechanical properties: tensile test results

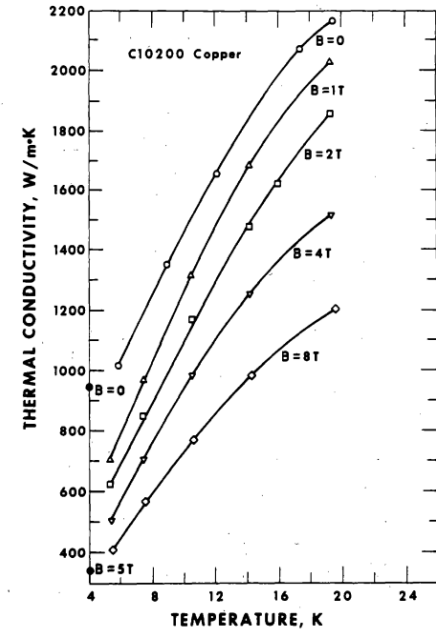
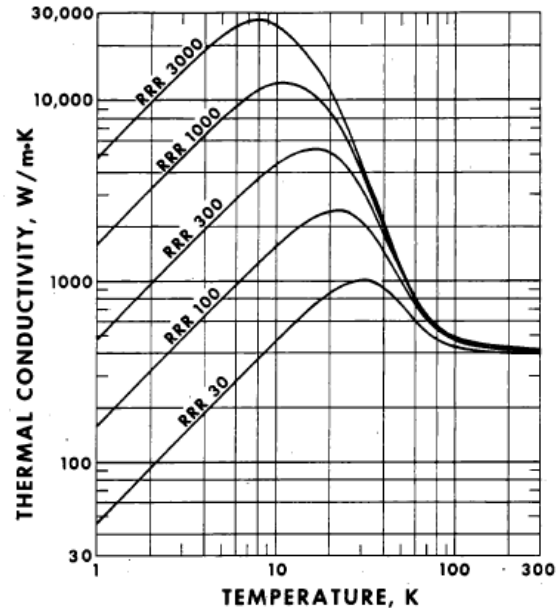
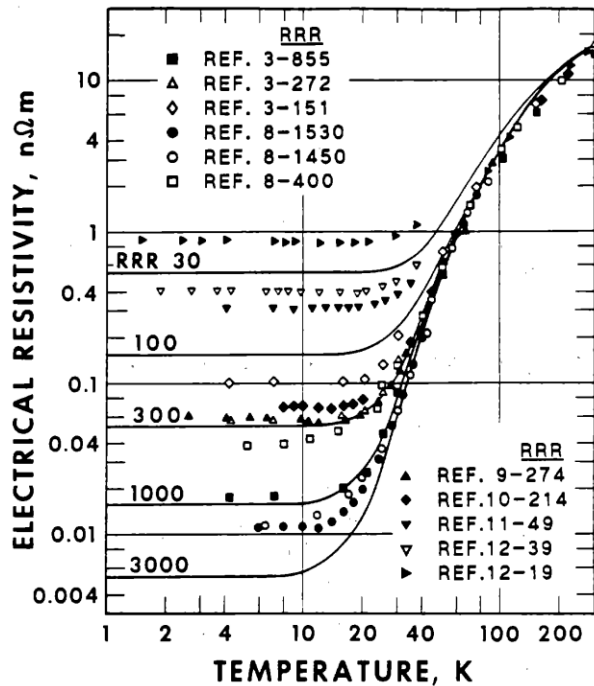


Temperature	Number of specimens	Young modulus	Yield strength	Ultimate strength	Deformation to rupture
[K]		[GPa]	[MPa]	[MPa]	[%]
293	3	330 +/- 11	696 +/- 18	944 +/- 2	9.2 +/- 1.1
77	3	320 +/- 40	-	1155 +/- 52	0.45 +/- 0.03
4.2	4	324 +/- 40	-	1048 +/- 53	0.34 +/- 0.03

[C. Garion et al., Material characterisation and preliminary mechanical design for the HL-LHC shielded beam screens operating at cryogenic temperatures, ICMC 2015]

Material properties

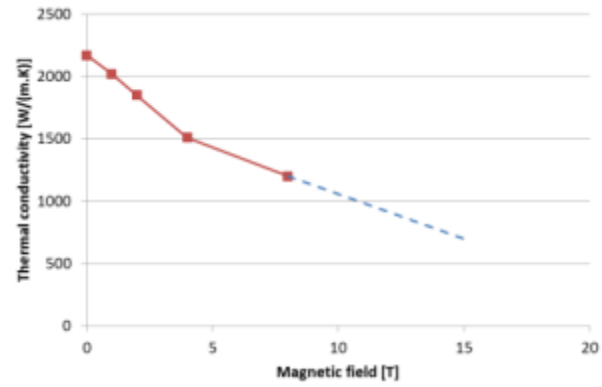
Copper



Thermal conductivity of copper

Properties have been defined for RRR \sim 100.

[N.J. Simon, E. S. Drexler, R.P. Reed, Properties of Copper and Copper Alloy at Cryogenic Temperatures, 1992]

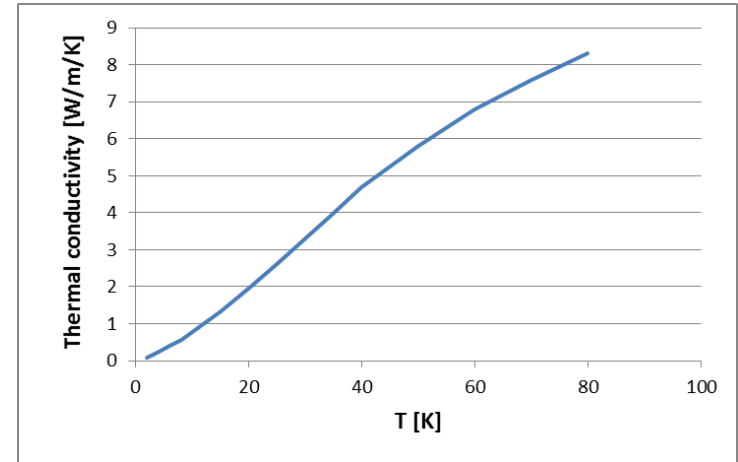


Material properties

Stainless steel*:

Electrical resistivity (50 K) $\sim 5 \cdot 10^{-7} \Omega \cdot m$

Thermal conductivity (50 K) $\sim 6 \cdot W \cdot m^{-1} \cdot K^{-1}$

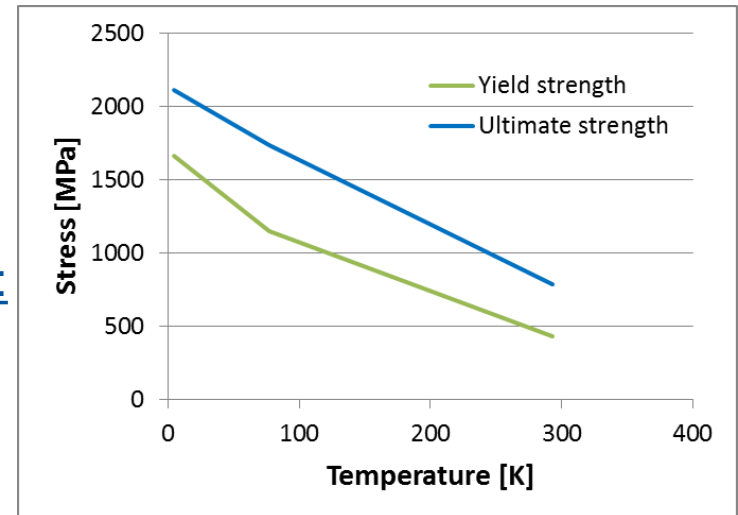


316LN:

Yield strength:

σ_y (4K)** ~ 860 MPa

σ_y (293 K) ~ 300 MPa



P506 (high-Mn high-N austenitic stainless steel):

Yield strength***:

σ_y (50K) ~ 1350 Mpa

Magnetic susceptibility $\sim 3 \cdot 10^{-3}$

P506 properties

*Jensen et al. Selected cryogenic data notebook, BNL, vol. 1

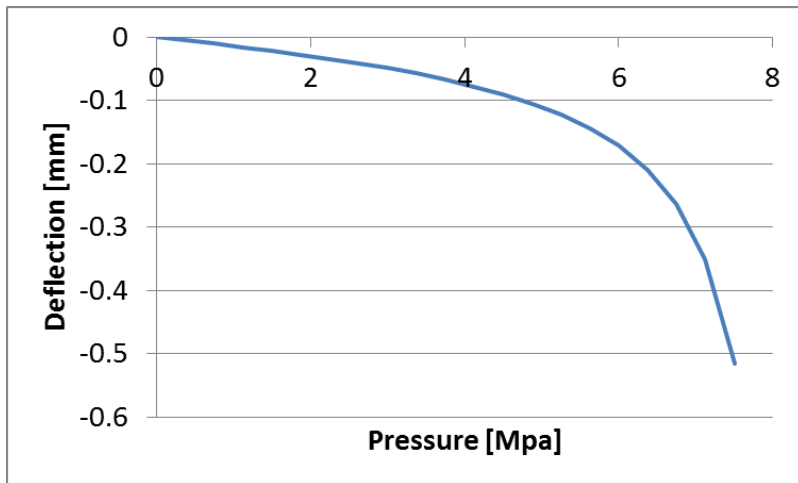
** Sa et al., Mechanical Characteristics of Austenitic Stainless Steel 316LN Weldments at Cryogenic Temperature, Fusion Engineering 2005

***Sgobba, S. and Hochörtler, G., A new non-magnetic stainless steel for very low temperature applications, Stainless Steel Science and Market, 1999; 2; 391-401

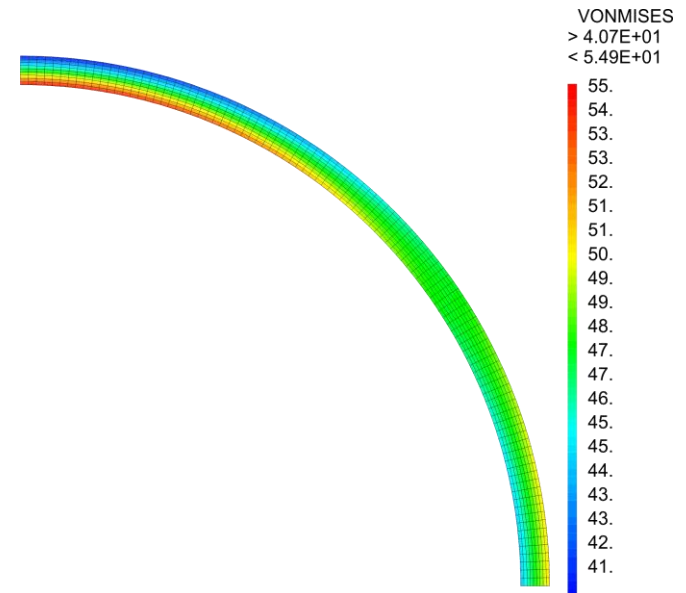
Mechanical design

The cold bore shall withstand an external pressure of 20 bars (design pressure).

According to standard EN13445-3 (Non fired pressure vessel), a thickness of 4 mm leads to a safety factor of 2.35.



Deflection of the cold bore tube under external pressure (nominal thickness 4 mm, non-circularity 0.1)

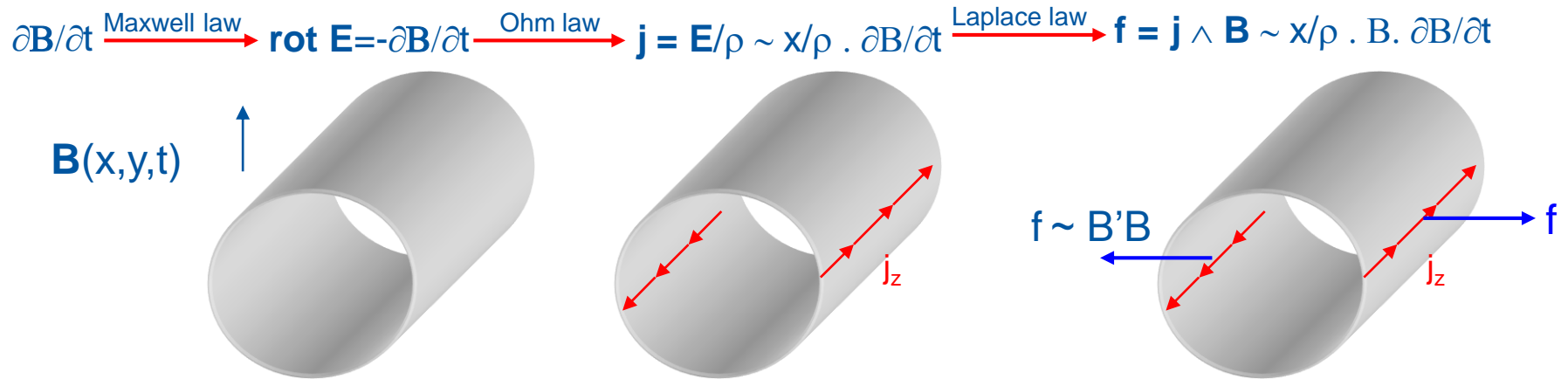


Von Mises stress profile during the pressure test at 25 bars

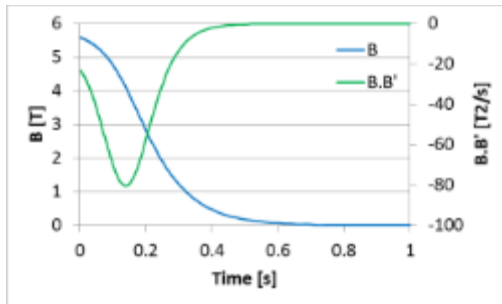
→ A minimum thickness of 4 mm is considered for the cold bore tube.

Mechanical design

The beam screen behaviour during a magnet quench is driven by the Foucault current:



Different aspects have to be considered for the analysis:

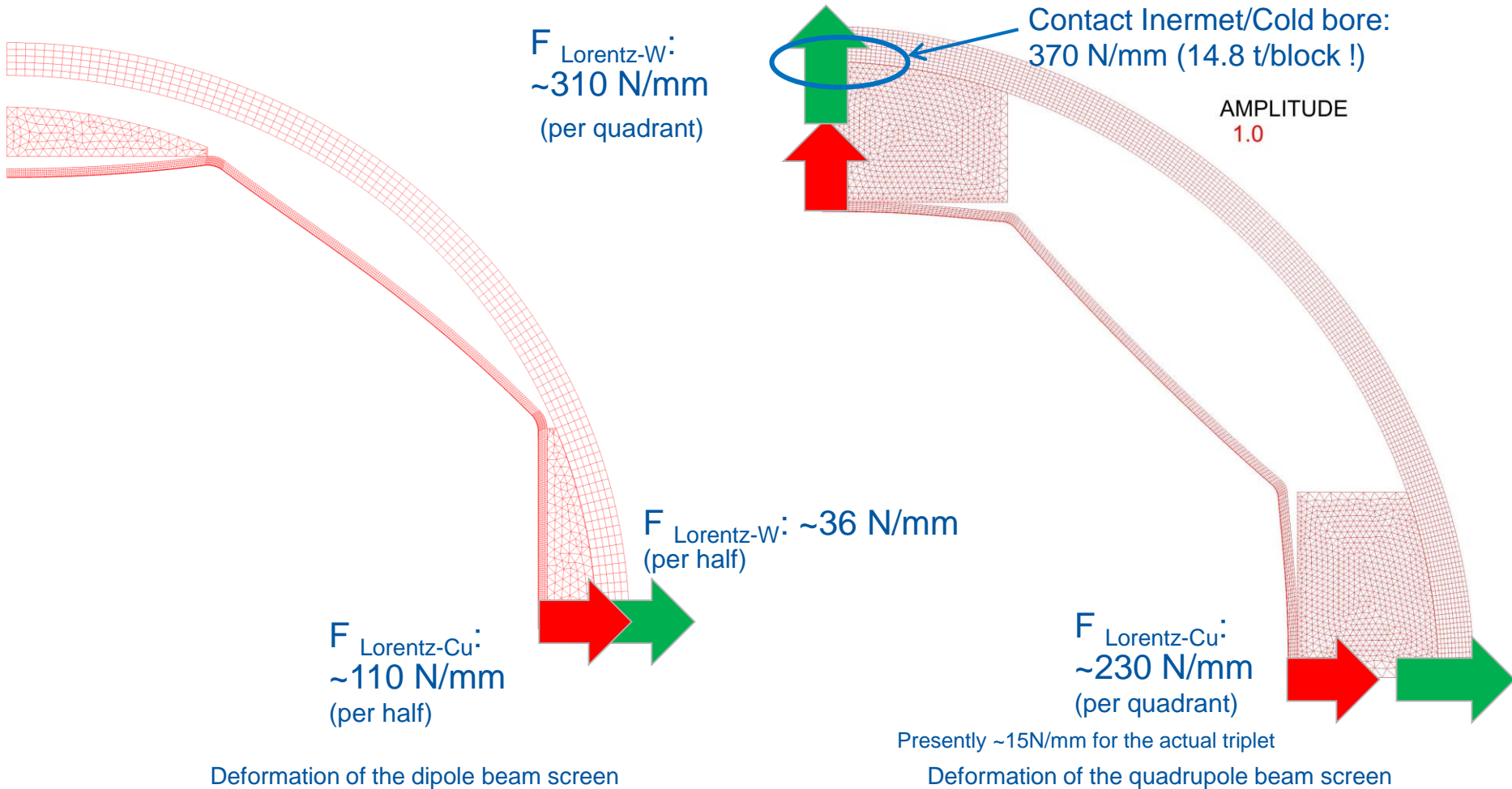


- $f=f(t)$
 - Quasi-static analysis
 - Dynamic analysis
- $\rho=\rho(T)$
 - Joule effect: $p = \rho \cdot j^2$

(Magneto-resistivity not considered in the study)

Mechanical design

Lorentz forces induced by Foucault currents:



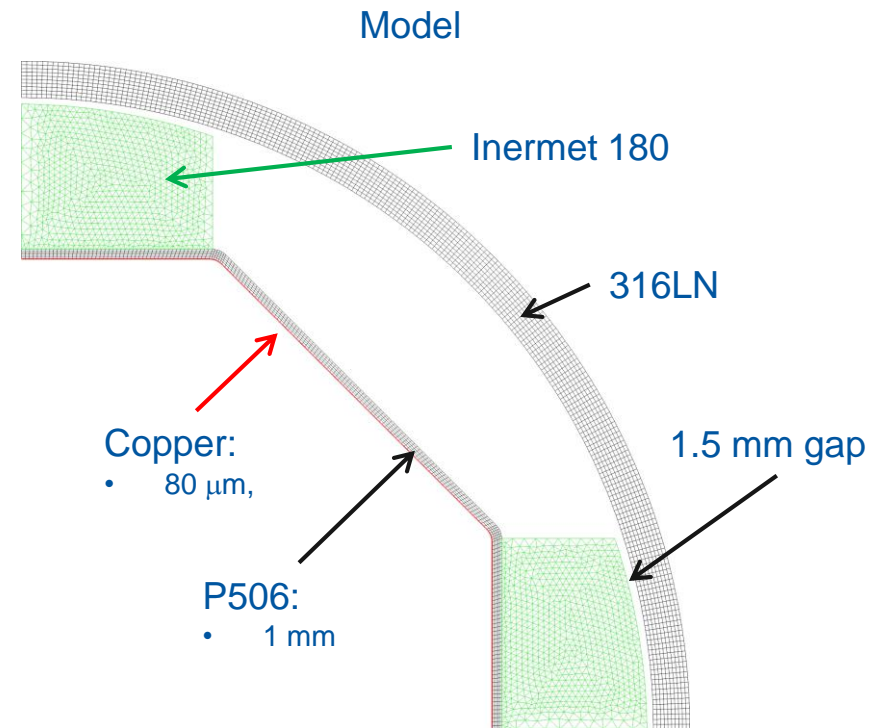
Mechanical design

Different beam screen models are used for the study of a magnet quench:

- 3D model is used to study the overall behaviour, validate the 2D assumption and study singularities (influence of thermal links, boundary effect,...)
- 2D model includes:
 - Fine mesh for the contact elements
 - Copper layer

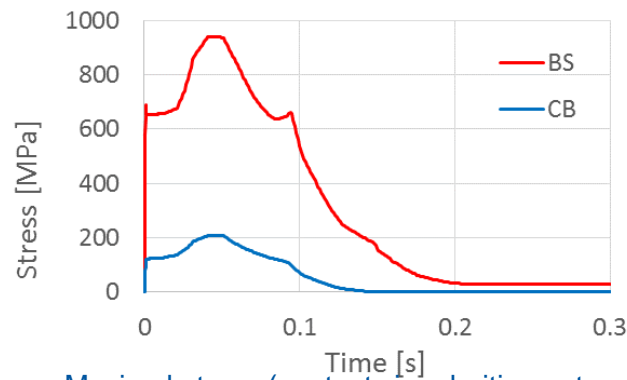
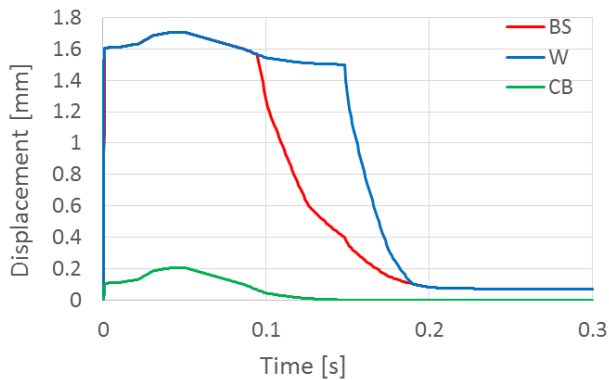
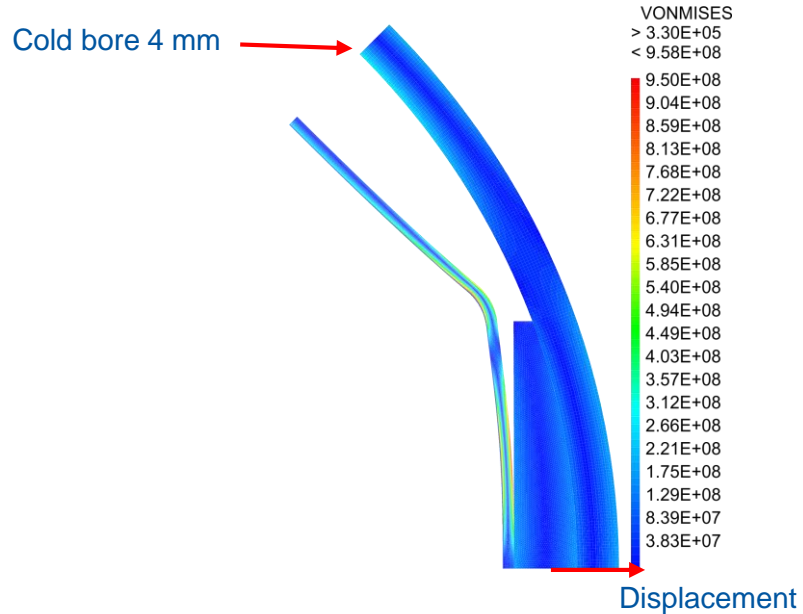
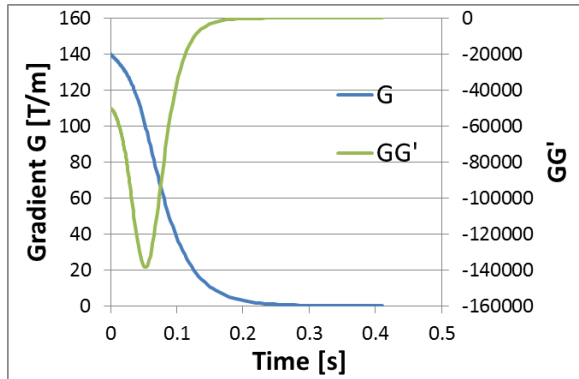
2D model doesn't consider neither the absorber extension nor the pumping holes.

Self-inductance of the beam screen is not taken into account.



Mechanical design

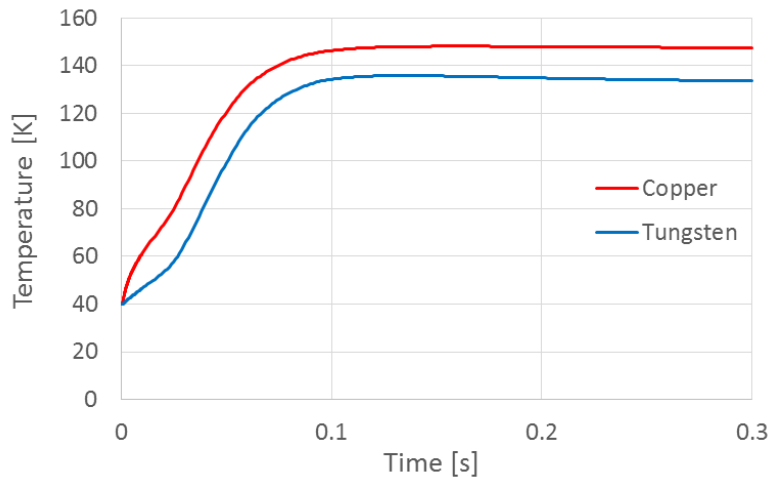
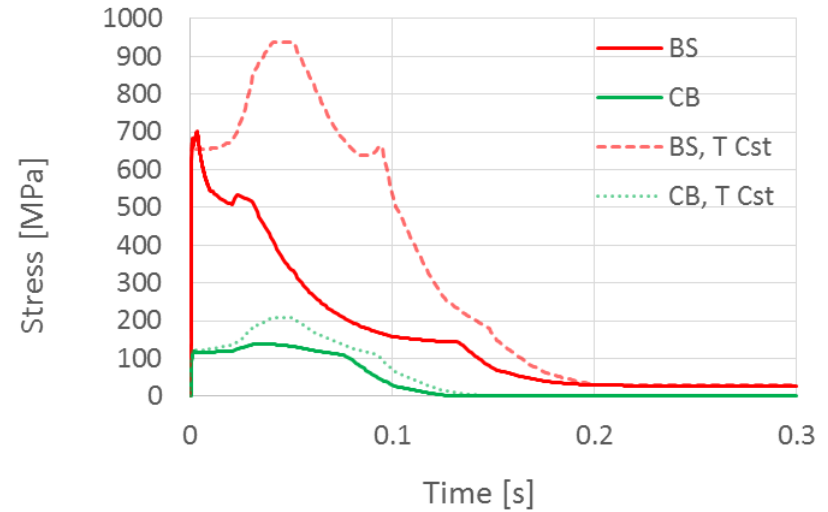
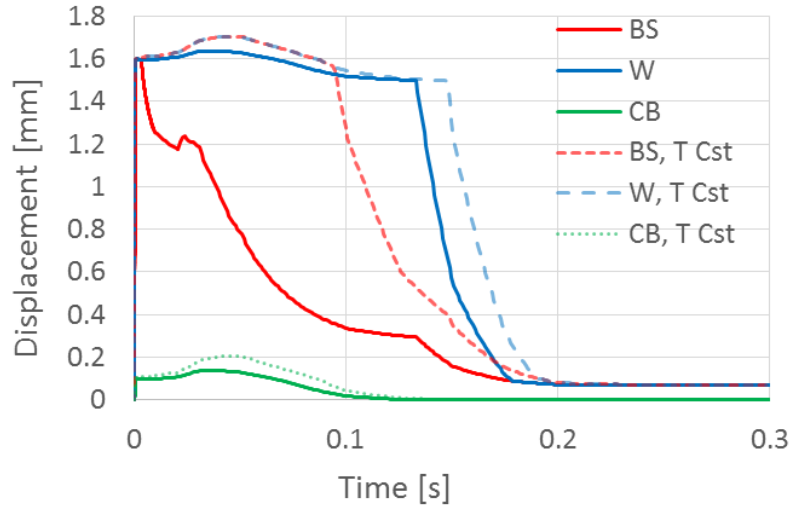
Q2-Q3 – Quasi-static analysis, constant temperature (40K)



Maximal stress (contact singularities not accounted)

Mechanical design

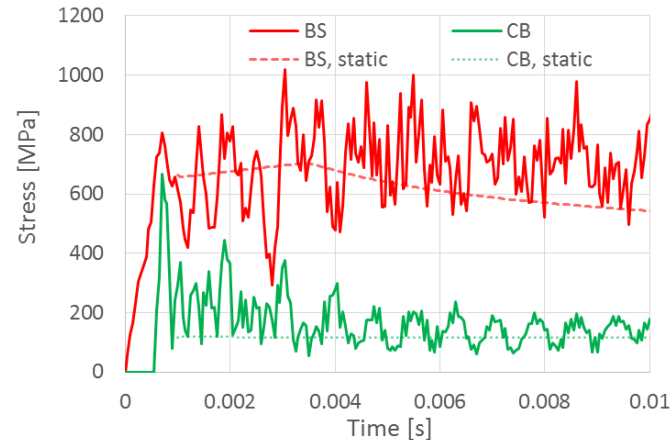
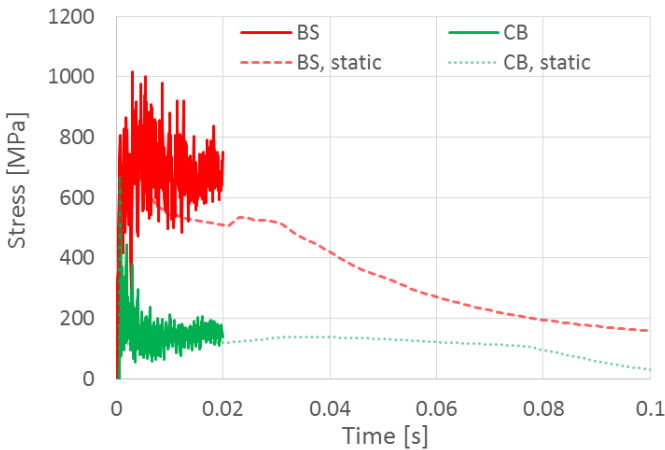
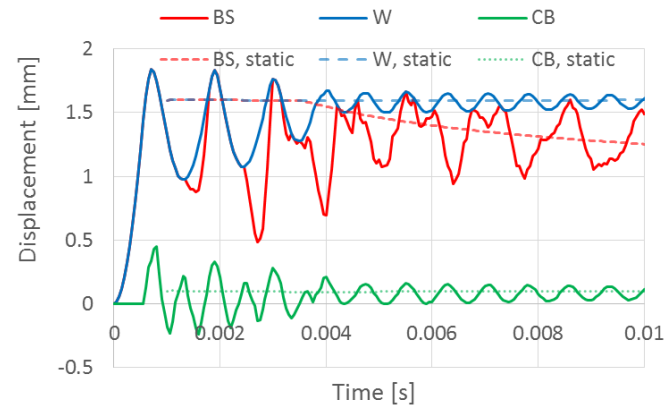
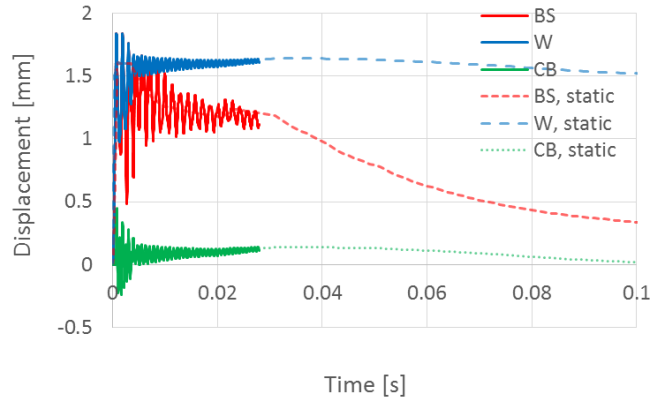
Q2-Q3 – Quasi-static analysis, Joule effect



→ Joule effect and the associated temperature increase has a significant impact.

Mechanical design

Q2-Q3 – Dynamic analysis, Joule effect

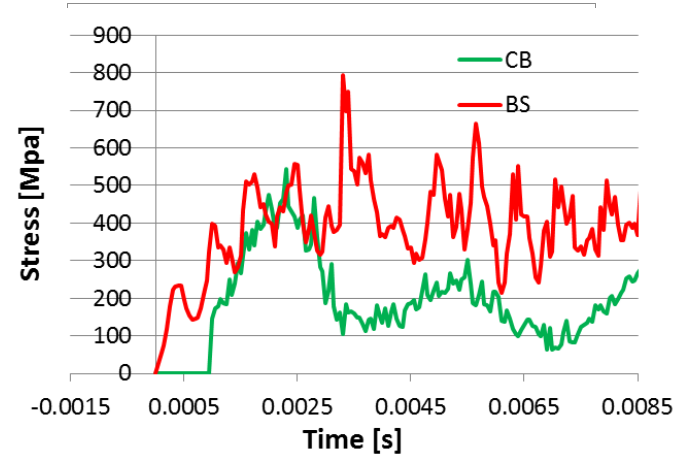
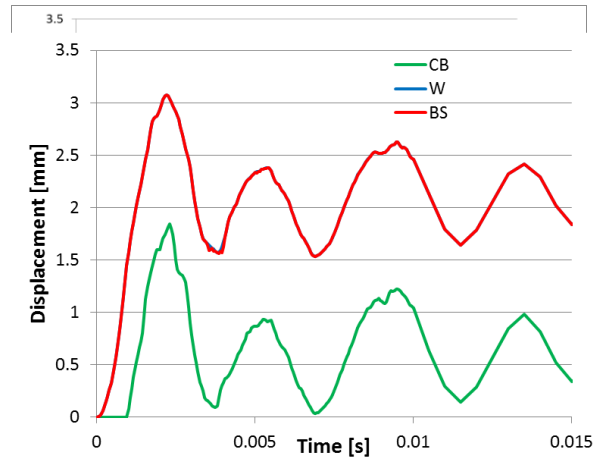


- Dynamic effects have a significant impact and shall be considered carefully.
- Present design for the Q2-Q3 fulfil the maximum stress and displacement requirements

Mechanical design

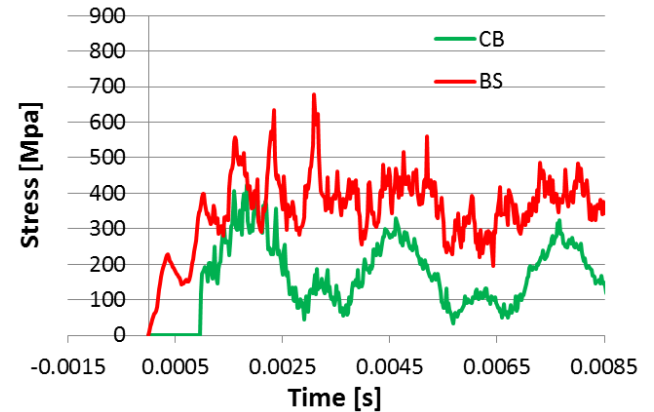
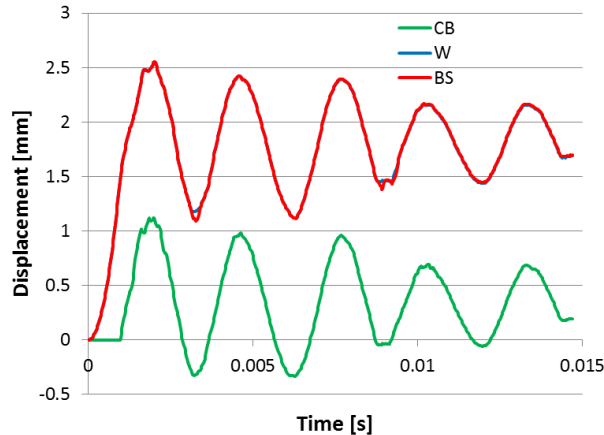
D1 – Dynamic analysis, Joule effect

Cold bore: 4 mm



→ Stresses are acceptable but displacement are too high (contact with the magnet coils).

Cold bore: 5 mm

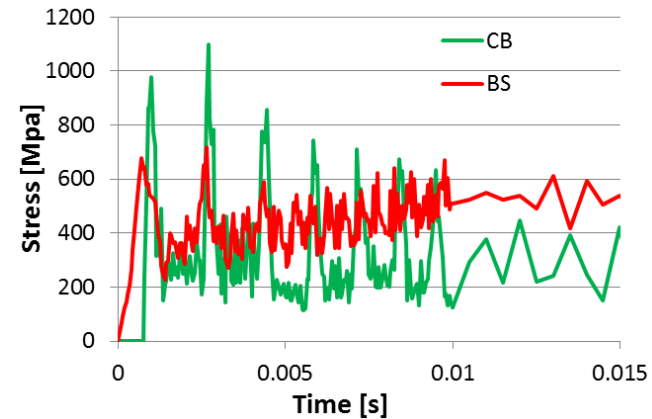
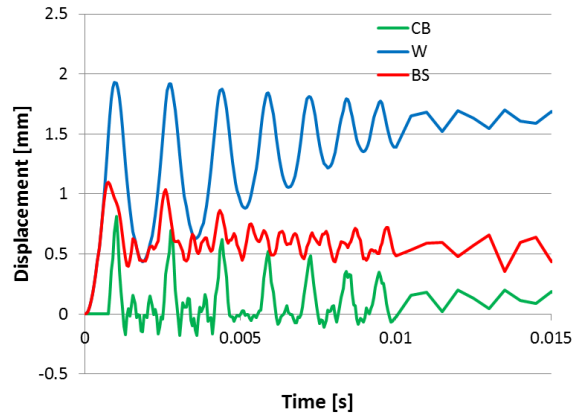


→ A cold bore of 5 mm is considered for D1.

Mechanical design

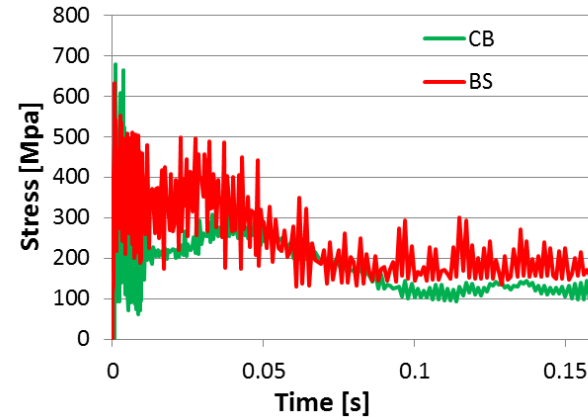
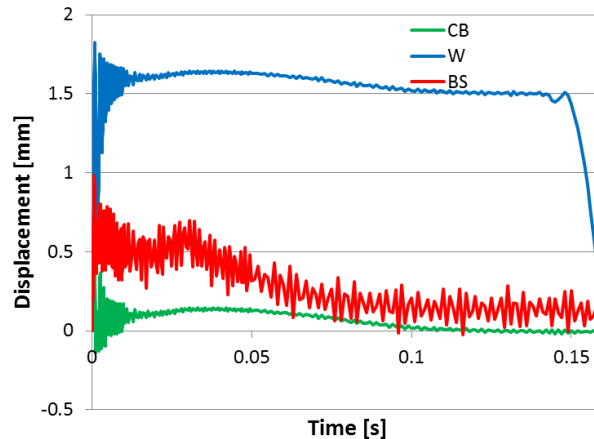
Q1 – Dynamic analysis, Joule effect

Cold bore: 4 mm



→ Stresses in the cold bore are not acceptable.

Cold bore: 5 mm



→ A cold bore of 5 mm is considered for Q1.

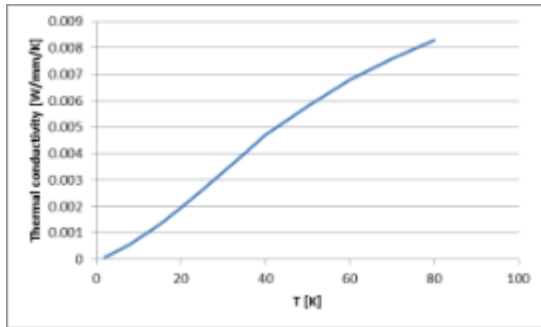
Heat transfer - Thermal link

Thermal analysis:

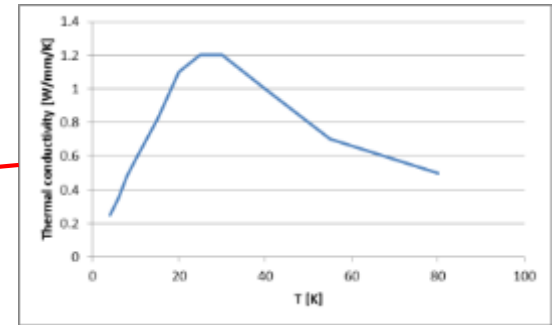
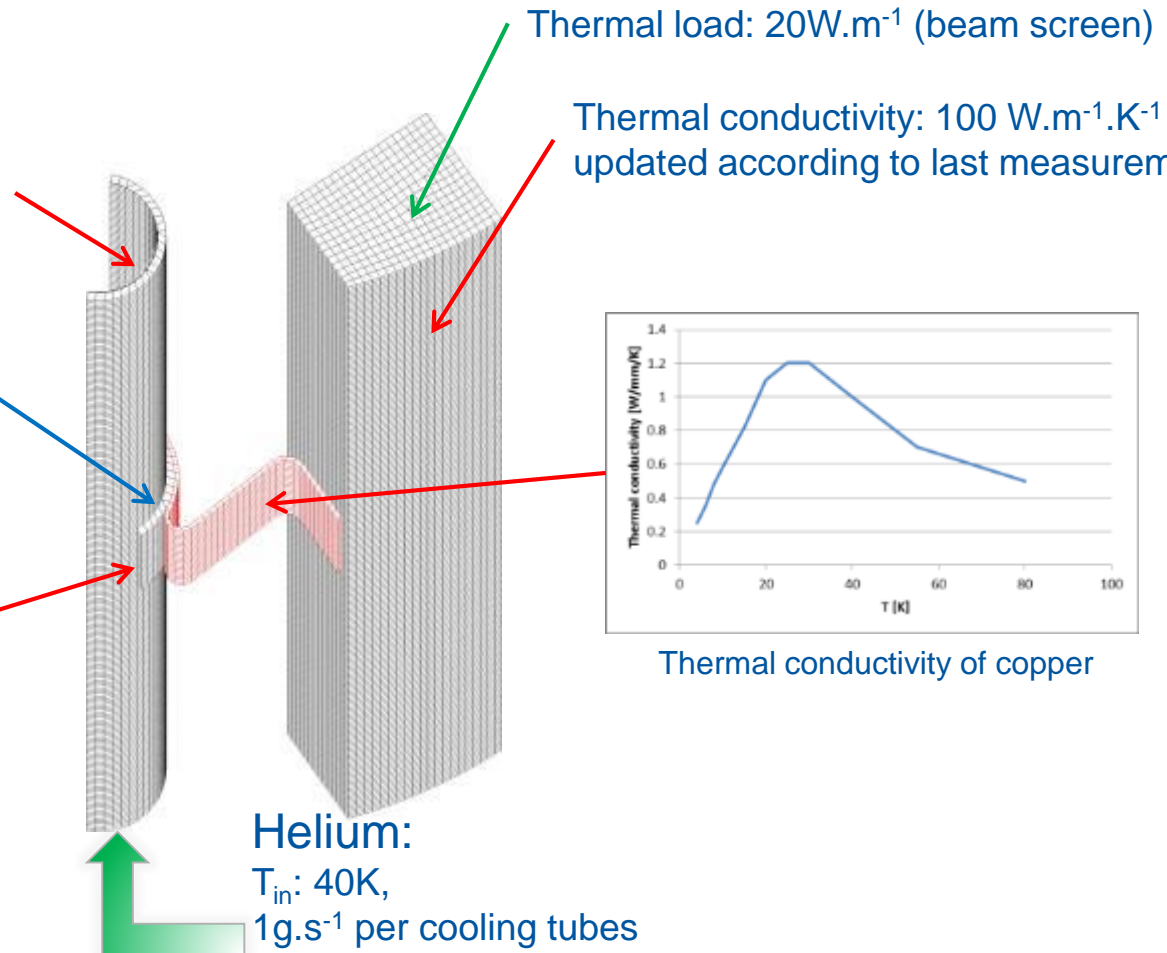
Convection heat transfer coefficient: $150 \text{ W.K}^{-1}.\text{m}^{-2}$

Values in the range 137-365 depending on estimation formulas (Colburn, Dittus-Boelter, Petukhov)

Welds on the 3 external edges



Thermal conductivity of P506



Thermal conductivity of copper

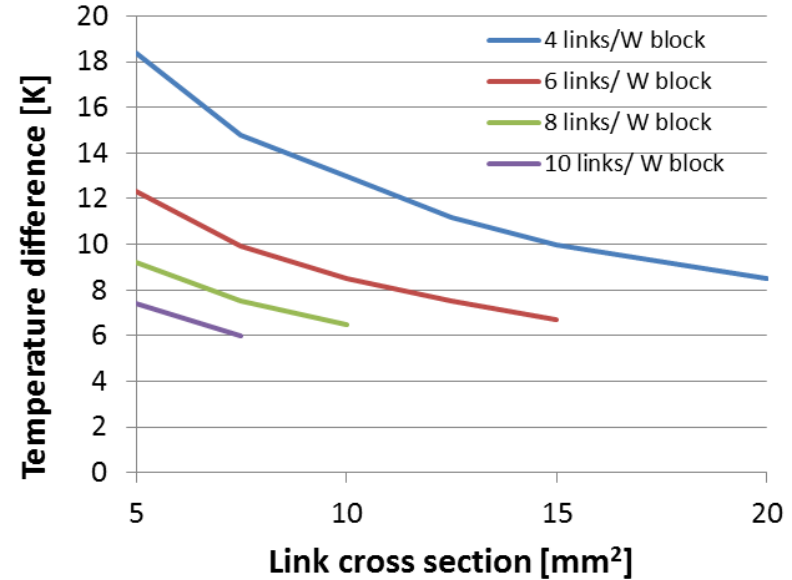
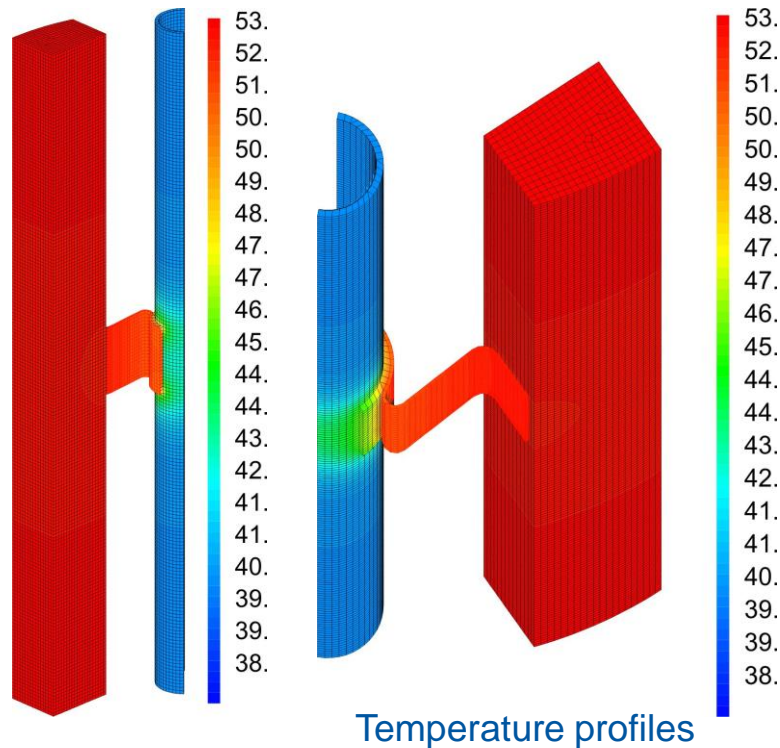
Helium:

$T_{in}: 40\text{K}$,

1g.s^{-1} per cooling tubes

Heat transfer - Thermal link

Thermal analysis:



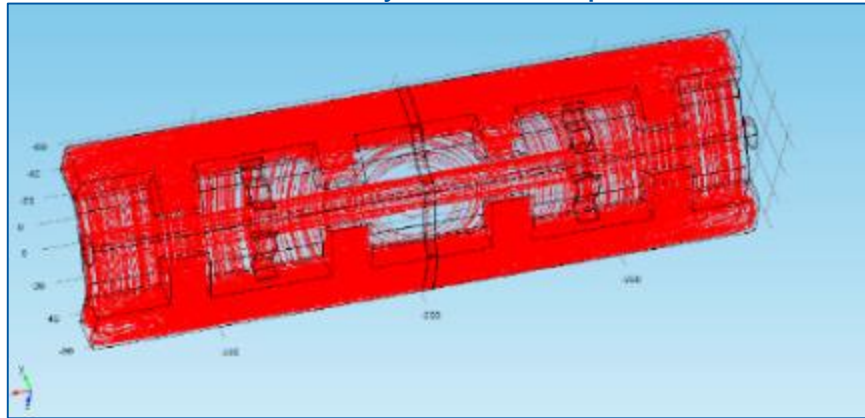
→ Present baseline is 6 thermal links, 10 mm² cross section, per block: $\Delta T \sim 8.5$ K
(Temperature gradient in helium: 0.5 K.m⁻¹)

→ Tests foreseen in 2016 with CERN cryolab.

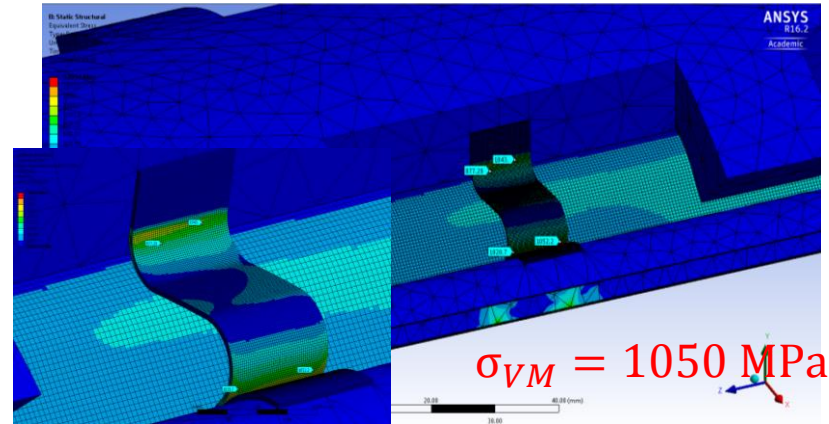
Heat transfer - Thermal link

Mechanical considerations:

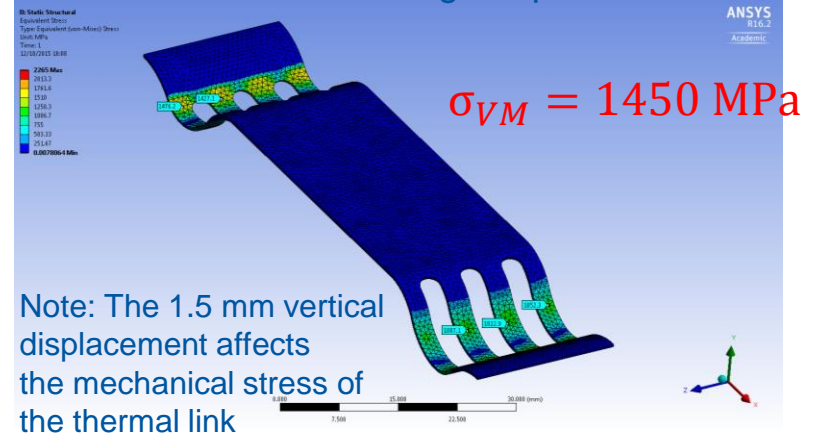
Eddy current loop



Stress induced in the S-shape thermal link



Stress induced in the wing-shape thermal link

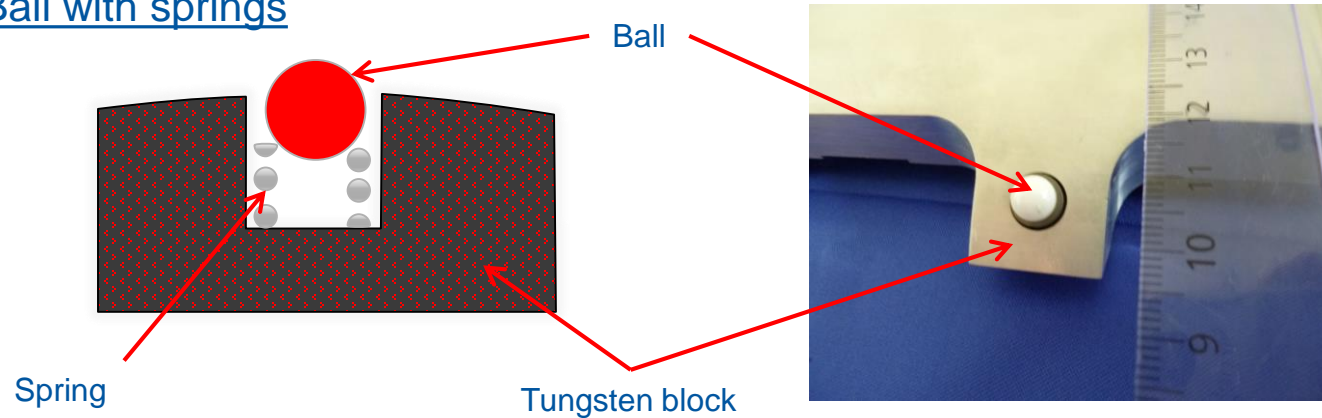


→ Design with a flat copper braid is under study.

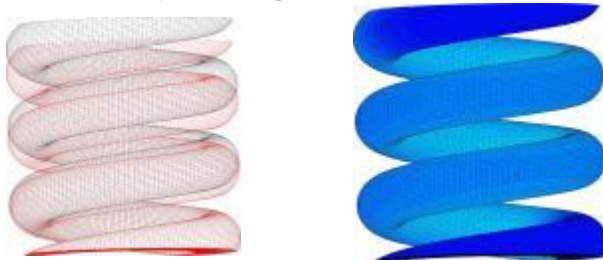
Heat transfer – supporting system

The supporting system has to be stiff enough to assure a good positioning but flexible enough to allow a uniform force transfer during a quench from the beam screen to the cold bore, while minimising the heat leak to the cold mass (0.5 W/m).

Ball with springs



Preliminary design (titanium)



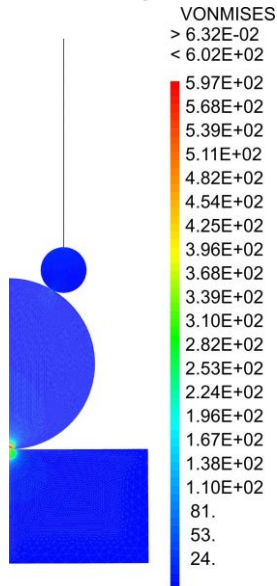
$D_e = 8$, $D_c = 1.6$, $h_0 = 7.3$ mm:

- Stiffness ~ 54 N/mm
- Maxi. compression ~ 2.5 mm
- Stress ~ 580 Mpa (1 mm compression)

Heat transfer – supporting system

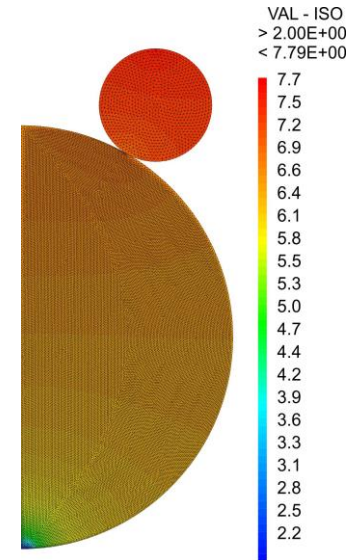
A solution based on zirconium oxide balls supported by elastic springs made of titanium alloy, grade 5, located in the Inermet® 180 absorbers is retained.

Mechanical analysis of the supporting system subjected to the weight of the beam screen.



- Local stress field
- Contact area between the components

Heat transfer evaluation from the warm beam screen to the cold bore



The heat leak to the cold mass through the supporting system is estimated conservatively (not thermal contact resistance) to be between 50 mW.m^{-1} and 400 mW.m^{-1} in the worst case, i.e. contact of the absorber and the first spring spire. Thermal conductivity of the ceramic at low temperatures has to be confirmed.

Nominal dimensions and tolerances

Cold Bore:

1. The coil inner radius at 1.9 K is 74.350 mm [P. Ferracin]
 - a. The insulated cable inner radius position at room temperature, with no stress, is 75 mm.
 - b. The deformation due to pre-load and cool-down is 0.400 mm
 - c. Quench heaters and insulation: 0.1 mm + 0.15
2. Gap coil/insulated cold bore at 1.9 K: 1.5 mm [R. Van Weelderen]
3. Cold bore insulation: 0.2 mm [P. Ferracin]
4. Tolerance on the cold bore thickness: 0/+0.5 mm

→ Nominal cold bore outer radius at 1.9 K: 72.15 mm

→ Nominal cold bore outer radius at room temperature: 72.35 mm

→ Nominal cold bore inner radius for Q1 and D1 (thickness 5 mm): 67.35 mm

→ Nominal cold bore inner radius for Q2 and Q3 (thickness 4 mm): 68.35 mm

Present specification based on a machined long circular tube: (Input's from Manufacture de forage, tbc)

- Inner diameter : 134.7 & 136.7 mm, tolerance: 0/+0.1
- Thickness: 5 & 4 mm, tolerance 0/+0.5
- Straightness: 0.3 mm/m

Nominal dimensions and tolerances

Cold Bore:

Results obtained on a short prototype (~1.2 m)

	Target for long cold bore	Specified	Obtained
Inner diameter	ID 0/+0.1	139 0/+0.063 (H8)	139 -0.003/+0.087
Thickness	t 0/+0.5	4 0/+0.25	4 -0.04/+0.085
Straightness	0.3 mm/m	0.3 mm/m	0.042 mm

Tungsten blocks (machined):

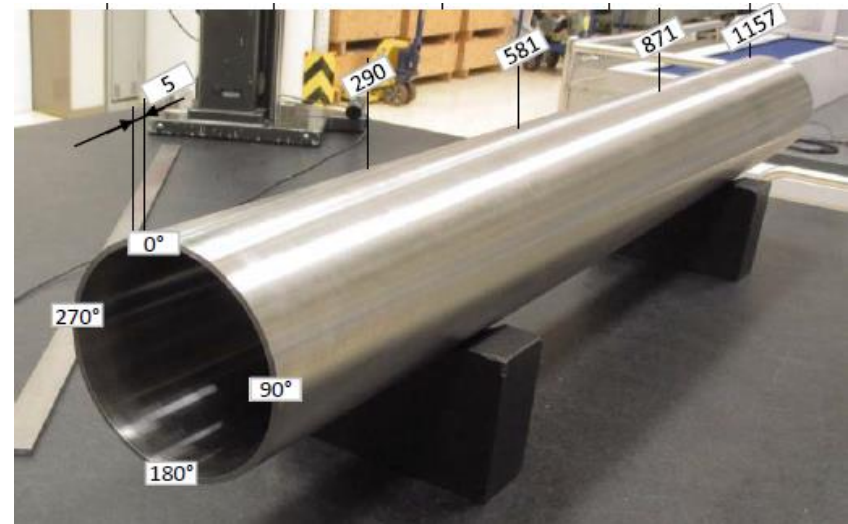
- Shape +/- 0.05

Ceramic balls:

diameter: +/- 0.0002

Titanium spring (3D printed):

+/- 0.1 mm ?



Nominal dimensions and tolerances

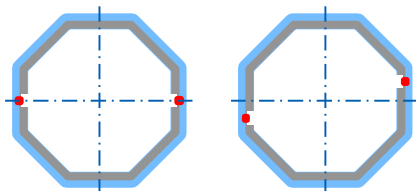
Beam screen:

Shape tolerance: +/- 1 mm (values from manufacturer)

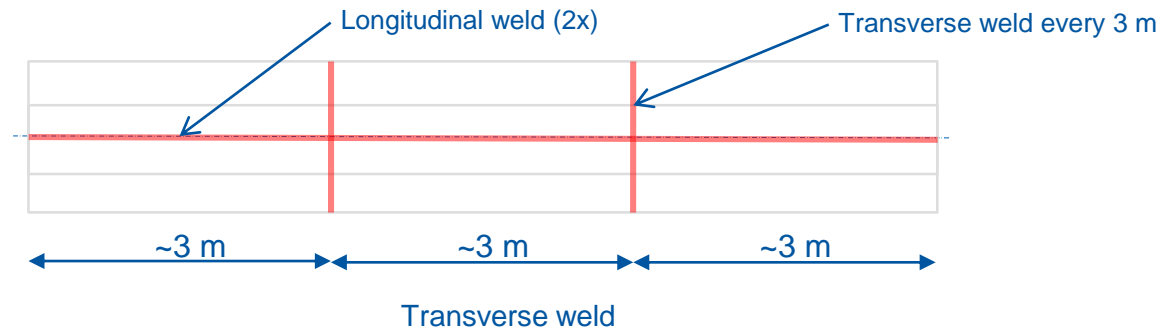
Measurement of the external dimension (nominal 104 mm) obtained on 2 short prototypes (1.2 m, 5 sections of measurements, 20 measures in total per screens):

	Beam screen 1	Beam screen 2
Minimal deviation	103.62	103.92
Maximal deviation	104.29	104.4
Standard deviation	0.22	0.15

Study of the impact of assembly welds on the impedance is ongoing. First results seem acceptable [B. Salvant].



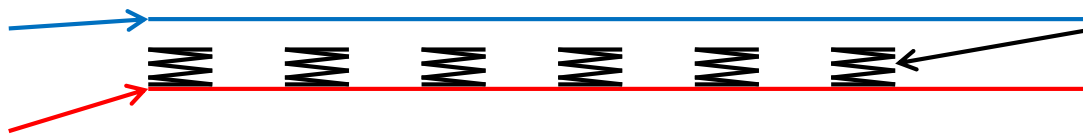
Longitudinal weld configurations (0/+90°)



Assembly tolerances

Beam screen;

- 1 mm thick, $I \sim 4.5 \cdot 10^5 \text{ mm}^4$
- 45 kg/m

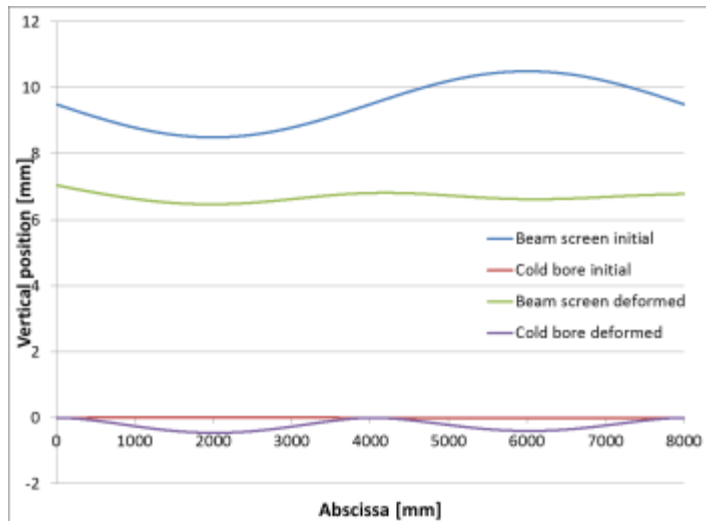


Spring:

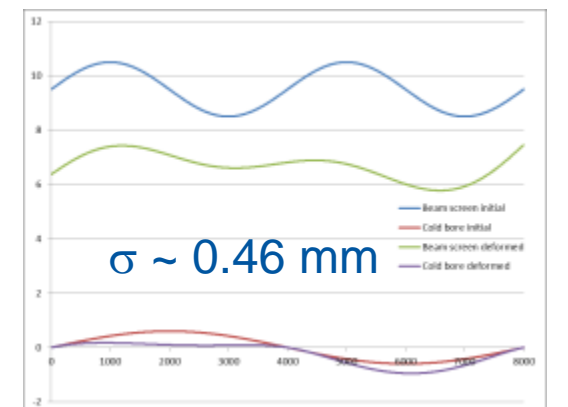
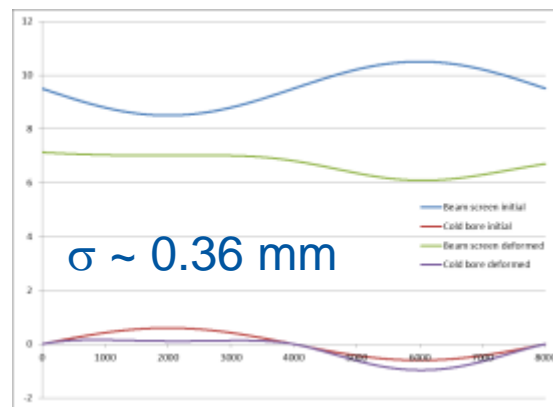
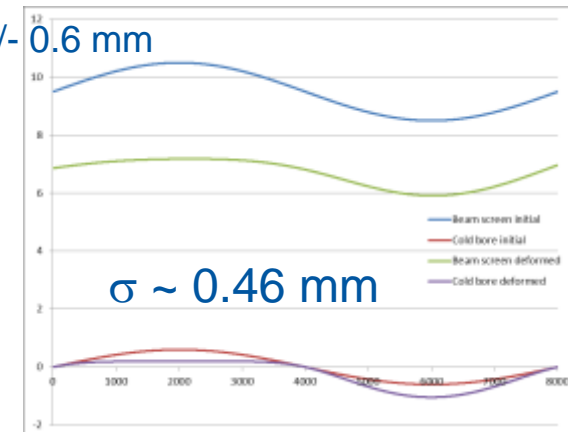
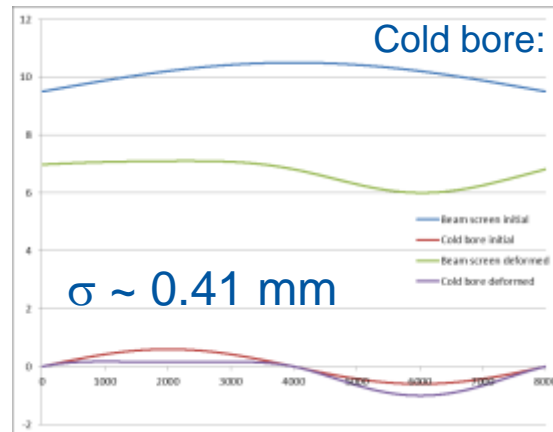
- 75 N/mm;
- every 10 cm
- Free length 7.5 mm

Cold bore;

- OD 147; 4 mm thick
- Clamped at the extremities, simply supported at the middle



“Perfect” cold bore, +/- 1 mm beam screen: $\langle y \rangle \sim 6.7 \text{ mm}$, $\sigma \sim 0.12 \text{ mm}$



Assembly tolerances

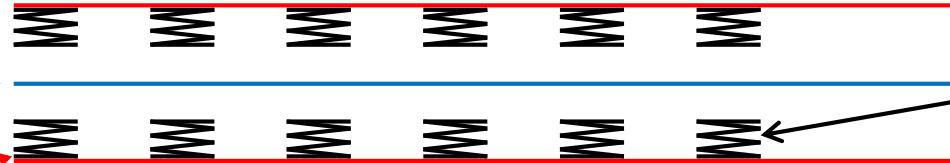
Vertical plane

Beam screen;

- 1 mm thick, $I \sim 4.5 \cdot 10^5 \text{ mm}^4$

Cold bore;

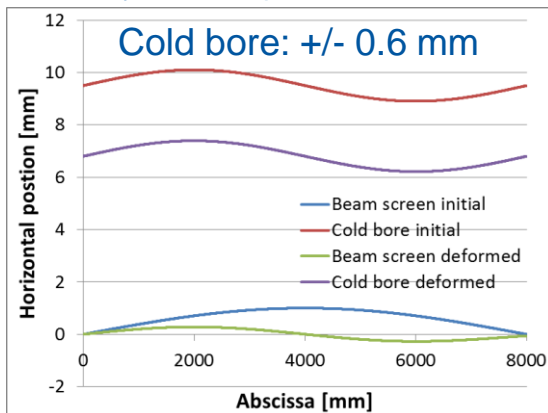
- OD 147; 4 mm thick
- Clamped at the extremities, simply supported at the middle



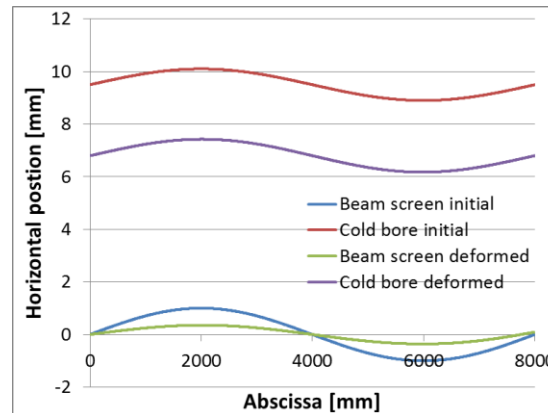
Spring:

- 37.5 N/mm;
- every 10 cm
- Free length 7.5 mm

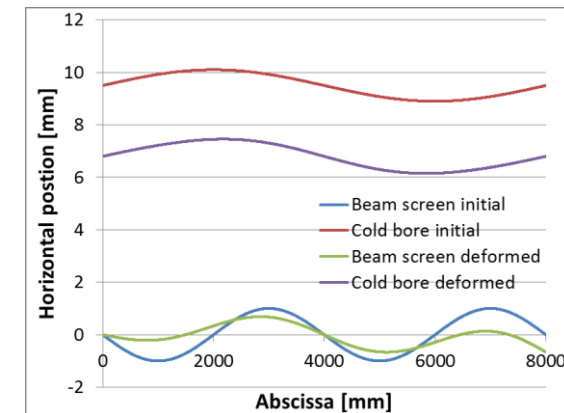
Arbitrary absolute position of cold bore



$\sigma \sim 0.2 \text{ mm}$



$\sigma \sim 0.25 \text{ mm}$

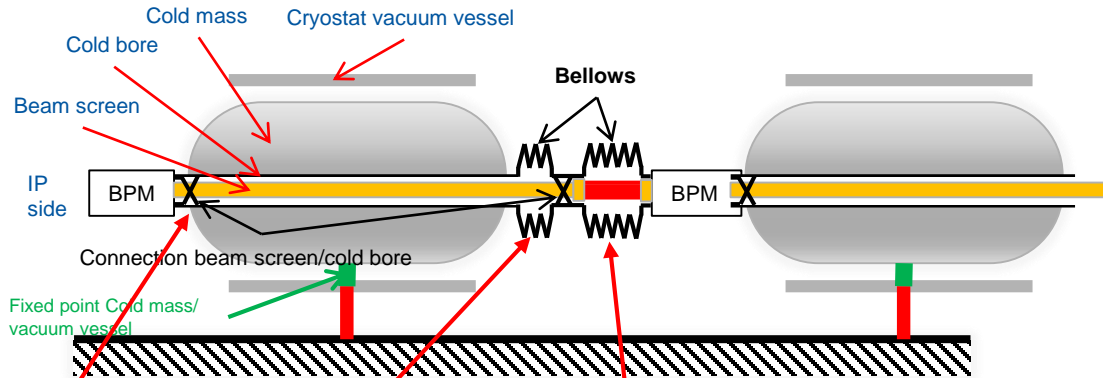


$\sigma \sim 0.4 \text{ mm}$

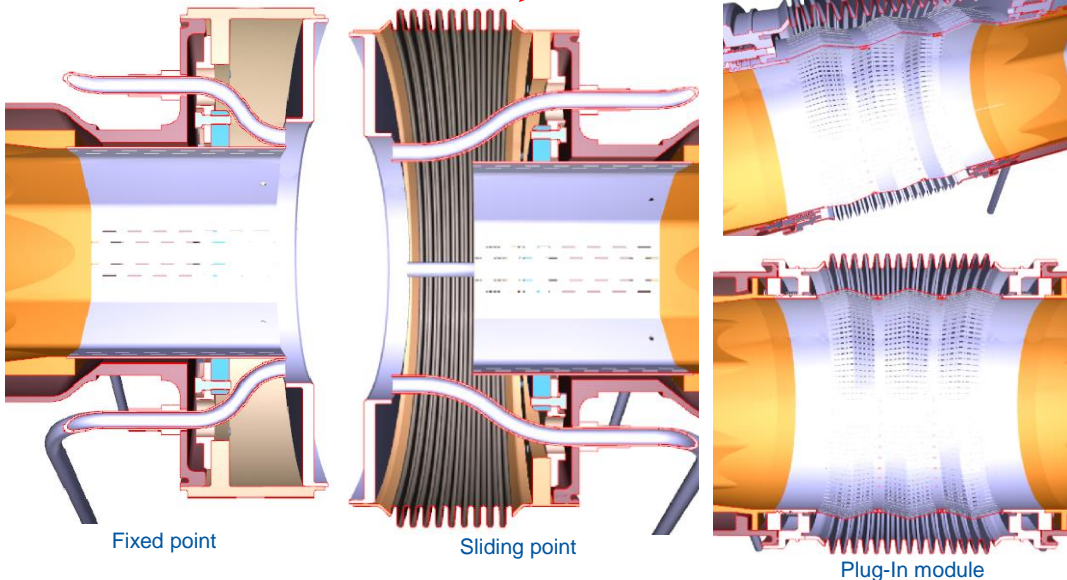
The standard deviation of the beam screen positioning is around 0.5 mm (in both planes).

Beam vacuum interconnection

Layout:



Preliminary design of the beam vacuum interconnections



Deformable RF finger prototype (not for the HL-LHC triplet interconnection)

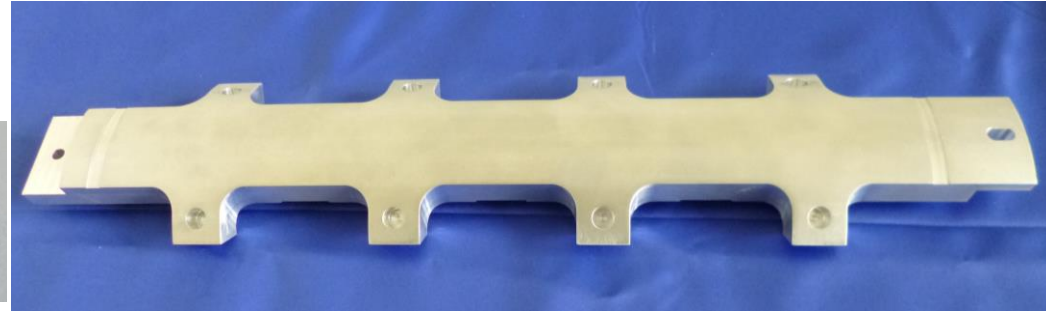


Prototyping

First short prototype (1.2m) has been assembled. Absorber blocks have been manufactured in aluminium.



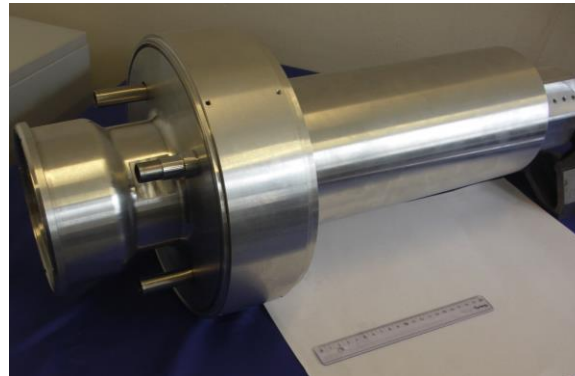
3D printed elastic ring and springs



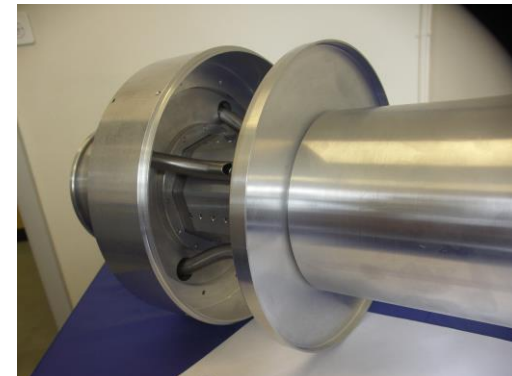
Absorber



Beam screen assembly

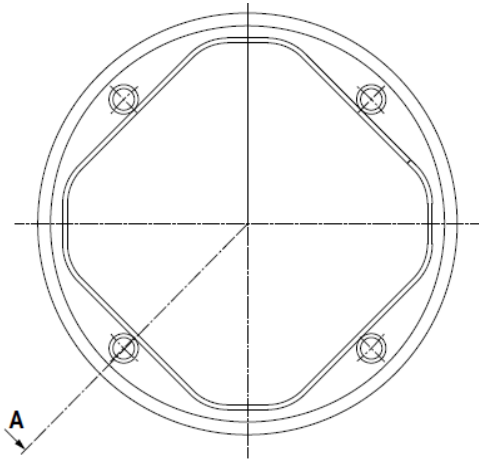


Beam screen/cold bore extremities

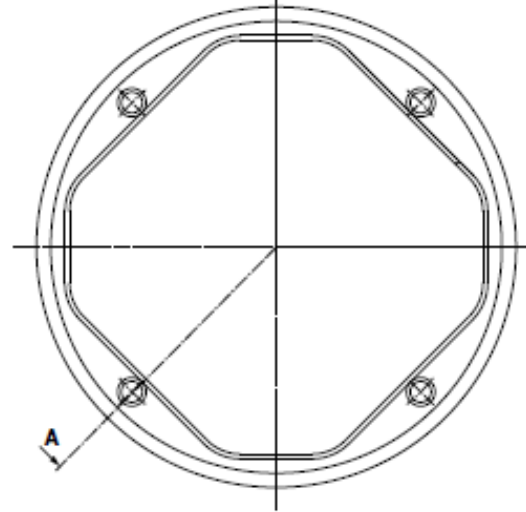


Stand alone magnet beam screen

Q4: octagonal shape, CB ID: 79.8

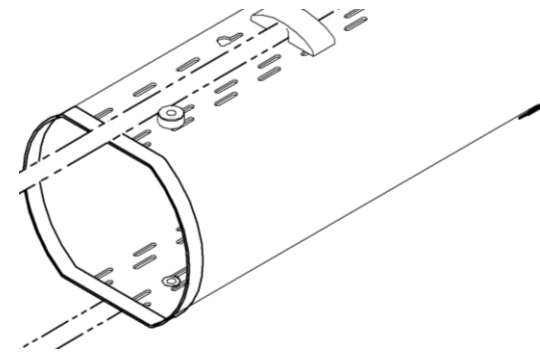


D2: octagonal shape, CB ID: 94



Similar design for Q4 and D2. Number of cooling tubes to be defined.

Q5, Q6 : racetrack shaped beam screen from old Q4 and Q5.



Summary

The design of the HL-LHC beam screen with shielding has been presented. It is based on a mechanical connection between the beam screen tube and the tungsten alloy blocks.

It integrates mechanical and thermal aspects while paying attention to the maximization of the aperture:

- Lorentz forces occurring during a quench are transmitted and absorbed by the cold bore. Dynamic effect and Joule heating have been taken into account.
- Heat load, absorbed by the tungsten blocks, are transferred to the cooling tubes via copper based thermal links,
- The beam screen is supported by ceramic balls to minimise heat load to the cold masses.

A study of the impact of the mechanical tolerances onto the aperture has been done. Tolerances have been measured on short prototype and values need to be confirmed with long prototypes.

Summary and next steps

Based on the last analysis, the following summary table of the main cold bore and beam screen parameters is considered.

	Cold bore		Beam screen 1 mm thick P506 *		
	Inner diameter	Thickness	Aperture H(V); +/-45 °	Cooling tube Nb * OD * thickness	Shielding maximum height
Q1	134.7 H8	5 0/+0.5	97.7; 97.7	4 * 16 * 0.8	16
Q2a	136.7 H8	4 0/+0.5	119.7; 111.7	4 * 10 * 0.8	6
Q2b	136.7 H8	4 0/+0.5	119.7; 111.7	4 * 10 * 0.8	6
Q3	136.7 H8	4 0/+0.5	119.7; 111.7	4 * 10 * 0.8	6
CP	136.7 H8	4 0/+0.5	119.7; 111.7	4 * 10 * 0.8	6
D1	134.7 H8	5 0/+0.5	117.7; 109.7	4 * 10 * 0.8	6
DFXJ	To be defined	~4 0/+0.5	To be defined	To be defined	-
D2	94	3 0/+0.5	86; 77	? * 6 * 0.8	-
Q4	79.8	2.6 0/+0.5	72.8; 62.8	? * 6 * 0.8	-

* the 80 µm copper layer not accounted.



Next steps

The design of the triplet beam screens has progressed significantly but still a lot of to do (non exhaustive list...):

Design & study:

- **Effect of the self-inductance of the beam screen**
- DFXJ beam screen/cold bore
- Update the design with wider absorbers
- Thermal links (geometry and assembly)
- Detailed stress analysis in the absorbers
- Plastic strain in the copper layer and assessment of the fatigue life (number of quenches)

Tests:

- Heat transfer tests (starting in 2016 with CERN cryolab)
- Assembly tests
- Quench tests?

Prototyping:

- Long cold bore prototypes (2* ~ 2.5m + 1 * ~ 9m)
- Short beam screen prototypes with correct materials
- Beam screen/cold bore extremities and interconnections

Manufacturing:

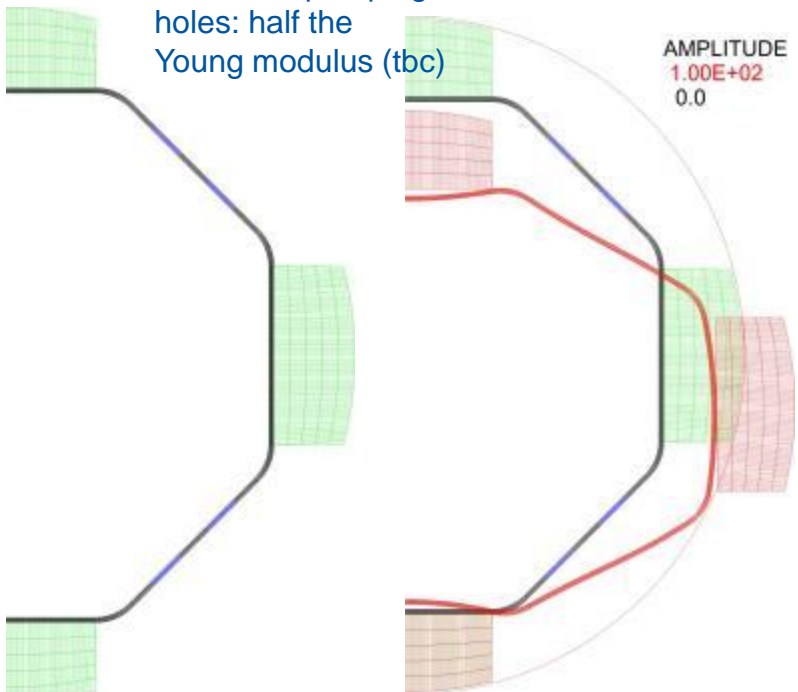
- Raw material order for the beam screen wall and cooling tubes
- Beam screen finishing facility



Gravity effect

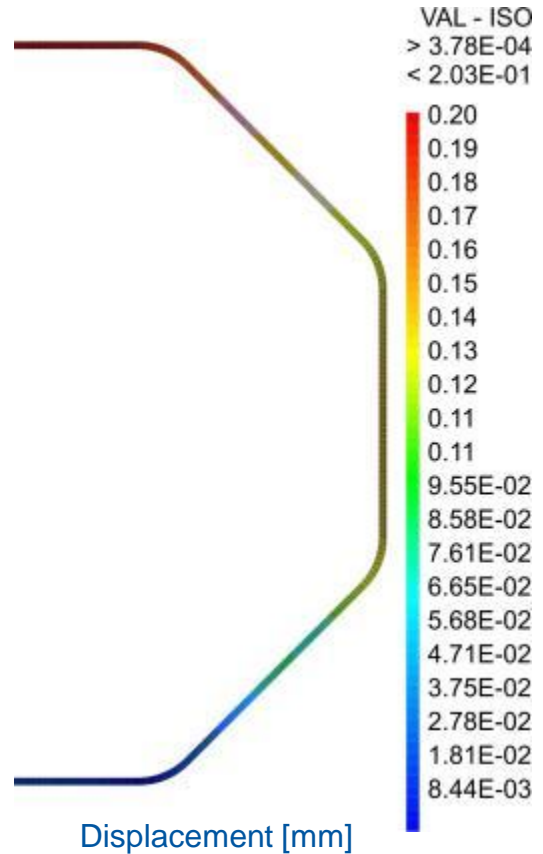
Self weight deformation (Q1 beam screen)
(no contact with cold bore)

Stiffness reduction
due to the pumping
holes: half the
Young modulus (tbc)

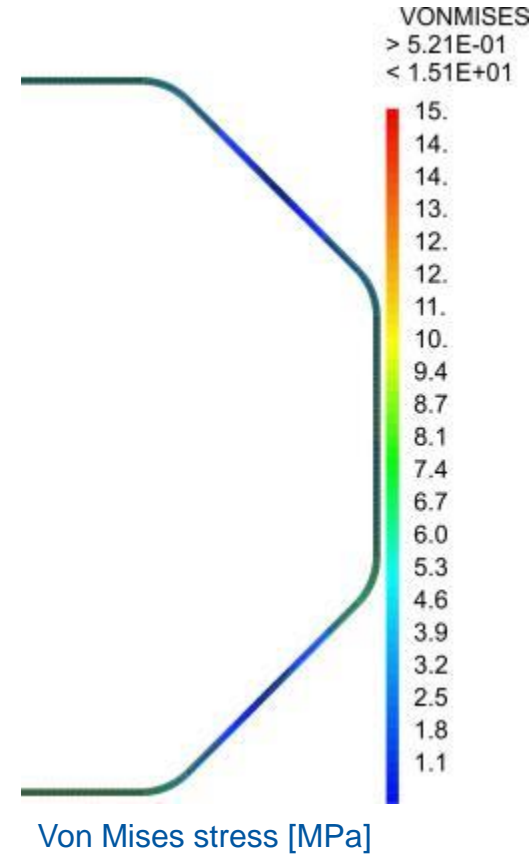


Deformed shape

AMPLITUDE
1.00E+02
0.0



Displacement [mm]



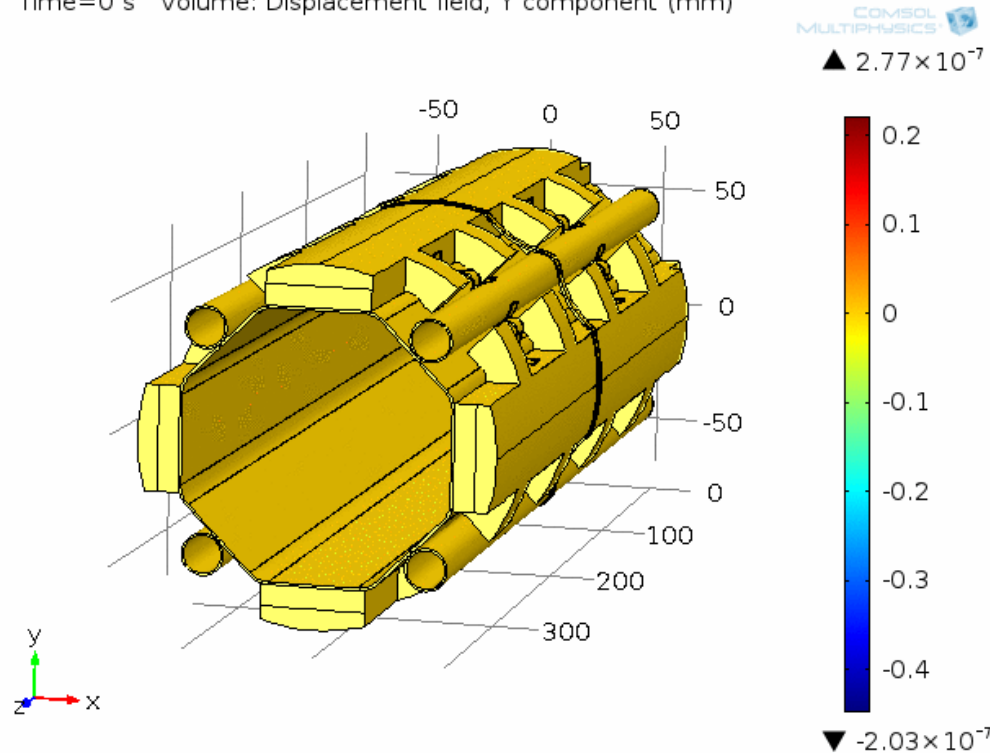
Von Mises stress [MPa]

Aperture reduction of 0.2 mm due to the gravity



Miscellaneous

Time=0 s Volume: Displacement field, Y component (mm)

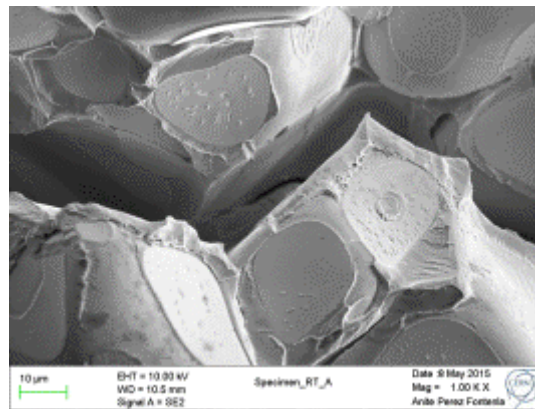
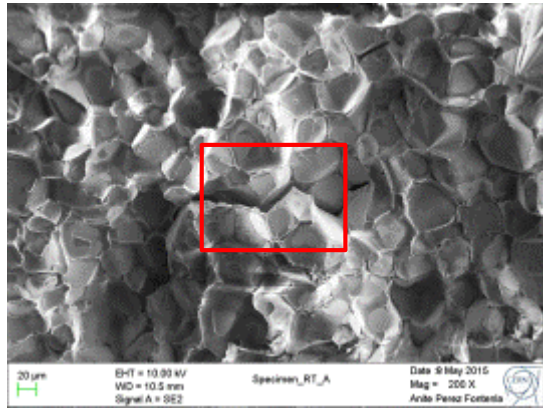


Animation to show at a glance how the beam screen gets deformed.

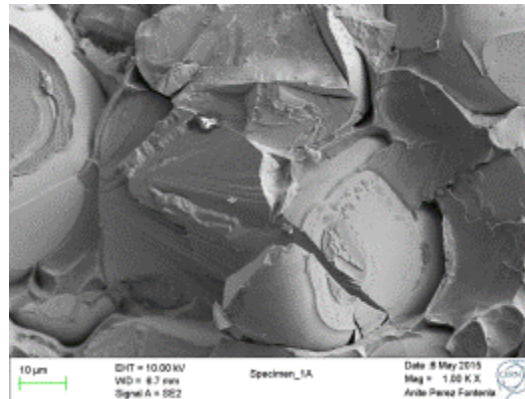
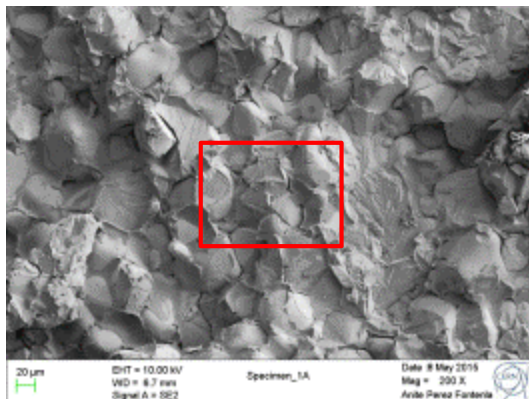
The contacts are not considered but it gives the idea of the whole deformations during a quench (quadrupole).

Fracture surfaces of Inermet® 180 after tensile tests

An intergranular fracture is observed on specimens tested at room temperature. Some microvoids and quasi-cleavage surfaces are noticed in the copper-nickel matrix. A few cleavages have been observed in the tungsten grains.

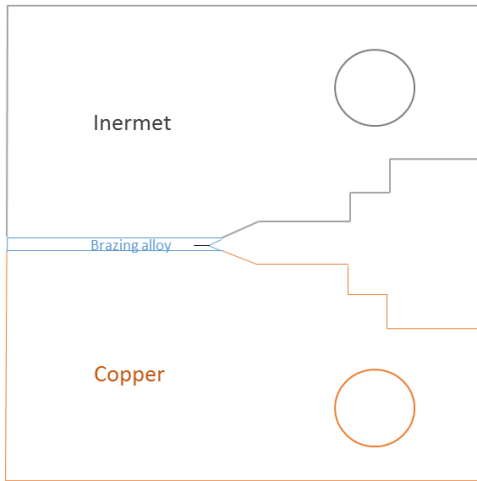


Examination of the fracture surfaces on specimens tested at 77 K revealed a transgranular brittle fracture dominated by cleavage in the tungsten grains. A debonding between them and the matrix is noticed as well.

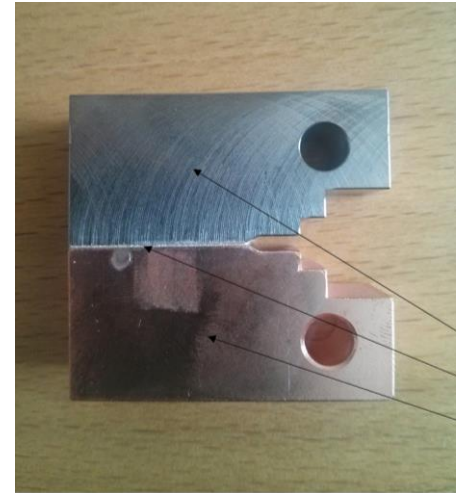


Fracture mechanics

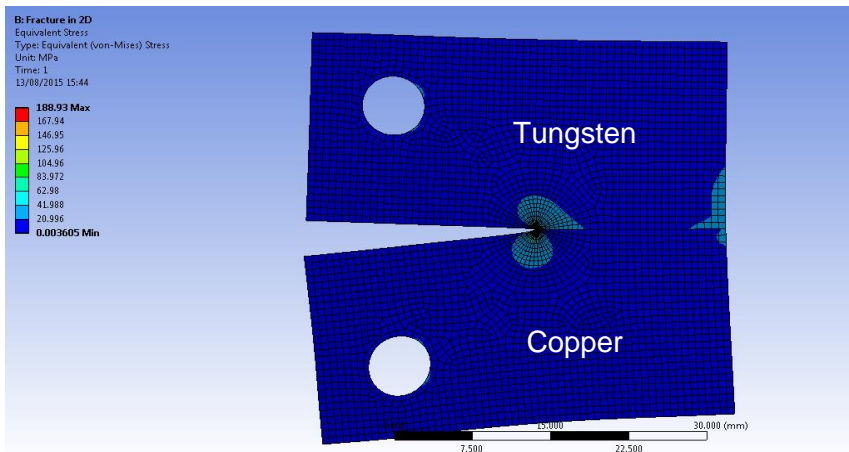
Mechanical considerations:



Vacuum brazing between copper and Inermet by means of an active brazing alloy (35.25 % Cu, 63 % Ag, 1.75 % Ti)



-INERMET 180
-Cusil ABA
-Copper



Crack size

12 mm

3.58E-03

-1.19E-02

delta [mm]

Force [N]

1.55E-02

100

compliance[mm/N]

1.55E-04

J integral [mJ/mm²]

cont 1

cont 2

cont 3

cont 4

cont 5

cont 6

7.36E-02

7.66E-02

7.66E-02

7.66E-02

7.66E-02

7.66E-02